Toxicology and Applied Pharmacology 239 (2009) 224–232

Contents lists available at ScienceDirect

Toxicology and Applied Pharmacology

journal homepage: www.elsevier.com/locate/ytaap

Influence of acid functionalization on the cardiopulmonary toxicity of carbon nanotubes and carbon black particles in mice

Haiyan Tong [a,*], John K. McGee [b], Rajiv K. Saxena [c], Urmila P. Kodavanti [b], Robert B. Devlin [a], M. Ian Gilmour [b]

[a] Human Studies Division, National Health and Environmental Effects Research Laboratory, US Environmental Protection Agency, Research Triangle Park, NC 27711, USA
[b] Experimental Toxicology Division, National Health and Environmental Effects Research Laboratory, US Environmental Protection Agency, Research Triangle Park, NC 27711, USA
[c] School of Life Sciences, Jawaharlal Nehru University, New Delhi 110067, India

ARTICLE INFO

Article history:
Received 23 April 2008
Revised 14 May 2009
Accepted 18 May 2009
Available online 27 May 2009

Keywords:
Acid functionalization
SWCNT
Carbon black
Cardiopulmonary toxicity
Mice

ABSTRACT

Engineered carbon nanotubes are being developed for a wide range of industrial and medical applications. Because of their unique properties, nanotubes can impose potentially toxic effects, particularly if they have been modified to express functionally reactive chemical groups on their surface. The present study was designed to evaluate whether acid functionalization (AF) enhanced the cardiopulmonary toxicity of single-walled carbon nanotubes (SWCNT) as well as control carbon black particles. Mice were exposed by oropharyngeal aspiration to 10 or 40 μg of saline-suspended single-walled carbon nanotubes (SWCNTs), acid-functionalized SWCNTs (AF-SWCNTs), ultrafine carbon black (UFCB), AF-UFCB, or 2 μg LPS. 24 hours later, pulmonary inflammatory responses and cardiac effects were assessed by bronchoalveolar lavage and isolated cardiac perfusion respectively, and compared to saline or LPS-instilled animals. Additional mice were assessed for histological changes in lung and heart. Instillation of 40 μg of AF-SWCNTs, UFCB and AF-UFCB increased percentage of pulmonary neutrophils. No significant effects were observed at the lower particle concentration. Sporadic clumps of particles from each treatment group were observed in the small airways and interstitial areas of the lungs according to particle dose. Patches of cellular infiltration and edema in both the small airways and in the interstitium were also observed in the high dose group. Isolated perfused hearts from mice exposed to 40 μg of AF-SWCNTs had significantly lower cardiac functional recovery, greater infarct size, and higher coronary flow rate than other particle-exposed animals and controls, and also exhibited signs of focal cardiac myofiber degeneration. No particles were detected in heart tissue under light microscopy. This study indicates that while acid functionalization increases the pulmonary toxicity of both UFCB and SWCNTs, this treatment caused cardiac effects only with the AF-carbon nanotubes. Further experiments are needed to understand the physico-chemical processes involved in this phenomenon.

Published by Elsevier Inc.

Introduction

Nanomaterials are being increasingly applied in a variety of industrial, medical and environmental settings. Engineered carbon nanotubes are a relatively new class of materials that are used as cosmetics and sunscreens (Aitken et al., 2006) as well as for systemic delivery of genes and drugs (Ajima et al., 2005; Bianco et al., 2005; Singh et al., 2006). Carbon nanotubes can be produced by different methods including combustion of fuels such as gasoline and diesel, and following controlled chemical synthesis and growth. Because of the high volume of production and widespread applications, nanotubes could become airborne and pose a potential inhalation health hazard, while their use in cosmetics and processing of food and water (Li et al., 2005) may result in dermal and oral exposures respectively. Therefore, there is an increasing need to evaluate the potential health hazards associated with exposure to these materials (Helland et al., 2007).

Carbon nanotubes have a strong tendency to aggregate into microscopic bundles, which in turn agglomerate loosely into small clumps or flakes that are mostly non-respirable (Lam et al., 2006). It has been shown that intra-tracheal instillation of high doses of SWCNTs in rodents causes inflammation, epithelioid granulomas, and fibrosis in the lungs and in some cases, blockage of the airways and cause asphyxiation (Lam et al., 2004; Stern and McNeil, 2008). In addition, pulmonary administration can also result in vascular toxicity and increased atherosclerotic lesions in ApoE$^{-/-}$ mice (Li et al., 2007).

Acid functionalization (AF) is a technique used to increase the solubility and dispersion of many different types of materials including nanotubes (Wang et al., 2006). Our previous study (Saxena et al., 2007) demonstrated that SWCNTs were highly agglomerated and did not disperse with prolonged sonication in normal saline solution. Acid functionalization of these particles resulted in highly dispersed suspensions in aqueous media which were more cytotoxic in mouse lung epithelial cell culture assays. Oropharyngeal aspiration of the AF-SWCNTs induced stronger pulmonary inflammation in mice than the non-functionalized material (Saxena et al., 2007), suggesting

* Corresponding author. 104 Mason Farm Rd, Chapel Hill, NC 27599, USA. Fax: +1 919 966 6271.
E-mail address: tong.haiyan@epa.gov (H. Tong).

0041-008X/$ – see front matter. Published by Elsevier Inc.
doi:10.1016/j.taap.2009.05.019

that either the chemical modification of the nanotubes or the degree and type of dispersion affected the toxicity of the carbon nanotubes (Wick et al., 2007).

Epidemiological studies have found associations between acute ambient PM exposure and adverse cardiac effects including cardiac ischemia, infarction, arrhythmia, and heart failure (Schulz et al., 2005). Since it has been shown that ultrafine ambient air pollution particles (PM) increase cardiac ischemia/reperfusion injury in mice (Cozzi et al., 2006) it is quite possible that carbon nanotubes may cause similar effects. Cardiac toxicity induced by PM is subtle in healthy animals, when assessed by EKG or cardiac histology since these methods only assess electrical and structural changes. The Langendorff cardiac perfusion method however allows the direct assessment of the indices of myocardial injury such as recovery of cardiac function and infarct size following ischemia/reperfusion injury. Therefore, this technique is a useful tool to assess functional cardiac changes after PM exposure.

In this study we hypothesized that pulmonary exposure to non-functionalized and AF-SWCNTs could cause cardiac impairment and that this response would be independent of pulmonary inflammation. Therefore we exposed mice to 10 μg or 40 μg of non-functionalized and AF-SWCNTs or LPS. To determine if acid functionalization could make laboratory-generated carbonaceous particles also more reactive, we also exposed mice to non-functionalized or AF-UFCB and compared the toxicity to SWCNTs.

Materials and methods

Experimental animals. Adult pathogen free female CD-1 mice (12 to 16 weeks of age, average body weight 30.8 ± 0.7 g) purchased from Charles River were used for this study. Once at the U.S. EPA Animal Care Facility (accredited by the Association for Assessment and Accreditation of Laboratory Animal Care), animals were housed in groups of five, provided a 12-hour light to dark cycle, maintained at 22.3 ± 1.1 °C and 50 ± 10% humidity, and given access to both water and *ad libitum*. Animals were acclimated for at least 10 days before the study began. The studies were conducted after approval by the EPA Institutional Animal Care and Welfare Committee.

Acid functionalization of particles. Single-wall carbon nanotubes (SWCNTs) were purchased from Sigma (catalogue #: 636797). Ultrafine carbon black particles (UFCB) were a gift from Dr. Vickie Stone, Napier University, Edinburgh, Scotland. Acid-functionalized SWCNTs (AF-SWCNT) and UFCB (AF-UFCB) were produced by suspending 20 mg of powder in 20 ml of 1:1 HNO_3:H_2SO_4 in 100 ml high-pressure vessels in a microwave digester as described previously (Saxena et al., 2007). Microwave power was applied at 50% of 900 W total and the pressure was controlled at 20 ± 2 psi for 3 min resulting in an internal temperature of 138–150 °C. Suspensions were cooled, diluted five-fold with H_2O and dialyzed four times against 5 l H_2O over a two day period. Dialyzed suspensions were dried by lyophilization, weighed and resuspended in 5 ml H_2O. At this stage the suspensions were black, well dispersed and had a neutral pH.

Chemical and physical characterization. Total carbon content of bulk solid samples was measured using a thermo-optical method (Sunset Laboratory, Tigard, OR; Birch and Cary, 1996). Agreement was within 12% of certificate analysis values for SWCNT and UFCB. Samples were ashed in quartz crucibles using a muffle furnace, with a programmed temperature of 100 °C–850 °C at 5 °C/min and then held at 850 °C for 30 min. Ash content was measured gravimetrically with subsequent digestion on a hotplate with aqua regia following US EPA Method 3050B. Elemental content was determined using Inductively Coupled Plasma-Optical Emission Spectrometry (ICP-OES) for 28 elements following US EPA Method 200.7 rev4.4 (Table 1). Sulfur content of the samples was lost by volatilization during the ashing process and not determined. A field-emission JEOL-2010f TEM (JEOL USA Inc., Peabody, MA) equipped with an Oxford EDS detector was used to examine the samples; the microscope was operated at 200 keV. All TEM images were recorded with a Gatan 794 slow-scan CCD camera (1024 × 1024 pixel array). Brunaeur–Emmett–Teller (BET) surface area measurements were made with a TriStar 3000 analyzer (Micromeritics Instrument Corporation, Norcross, GA). A Zetasizer Nano ZS (Malvern Instruments, Malvern, UK) was used for measuring particle size distributions of 20 μg/ml suspensions of AF-SWCNT and AF-UFCB in deionized water. SWCNT and UFCB suspensions were highly agglomerated and did not disperse sufficiently for particle size measurement.

Table 1
Elemental and ash content, surface area of nanoparticles.

Sample I.D.		SWCNT	AF-SWCNT	UFCB	AF-UFCB
Elemental content, μg/g (average, $n=4$)	C	849,500	685,400	912,800	439,500
	Al	117	186	24	701
	Ca	569	1060	18	1387
	Co	7600	5760	<5	<5
	Cr	1810	1210	<5	<5
	Fe	891	641	9	151
	Mg	92	83	<2	134
	Mn	70	53	<5	10
	Mo	2340	464	<10	<10
	Ni	181	134	<5	17
	SiO2	307	603	37	417
	Zn	9	113	<5	910
	Total	863,500	695,700	912,900	443,200
Ash content, surface area (average, $n=2$)	Gravimetric ash content, μg/g	24000	6000	9000	4000
	BET surface a rea, m^2/g	325	93	230	2

Gravimetric ash content determined after ashing. Inorganic elemental contents determined after ashing and aqua regia digestion. The concentrations of Ag, As, B, Ba, Be, Cd, Cu, Li, P, Pb, Sb, Se, Sn, Sr, Ti, Tl, and V were <10 μg/g in all samples.

Particle exposures. The biological effects of aspiration are shown to be comparable to the inhalation route exposure. A recent study by Shvedova et al. (2008) has demonstrated that the pulmonary toxicity of inhalation exposure to respirable SWCNT were very similar to those seen after pharyngeal aspiration route of SWCNT in mice. The concentration of particles and time point selected for this study were similar to those used in our previous study (Saxena et al., 2007). The particles were sonicated for 5 s at a setting of 4/10 in ice using an ultrasonic cell disruptor (Misonix Inc. Farmingdale, NY) prior to animal exposure. Mice were anesthetized by isofluorane vapor inhalation and instilled via involuntary aspiration with a 50 μl saline bolus containing 10 or 40 μg of particles, 2 μg of LPS (Sigma Chemicals, St. Louis MO), or with saline control as described previously (Gilmour et al., 2004).

Necropsy. Our previous study (Saxena et al., 2007) has shown that AF-SWCNT resulted in significant pulmonary inflammation 24 h after exposure. Therefore, mice from each group were anesthetized with sodium pentobarbital 24 h after particle exposure. Blood was drawn in a syringe and heparinized. A complete blood count (CBC) was obtained using a Hematology Analyzer (Coulter Inc., Miami, Fl) and the plasma was immediately stored at −80 °C and later analyzed for coagulation and inflammation markers. The trachea was exposed and cannulated, the thorax was opened and lung lobes were lavaged 3 times with 35 ml/kg sterile saline. The resulting bronchoalveolar lavage fluid (BAL) was stored at −80 °C and later analyzed for biochemical markers of lung injury and edema. Total cell counts in the BAL were obtained with a coulter counter. The remaining sample was centrifuged in duplicate onto slides and stained with DiffQuik solution (American Scientific, PA) for cell differentials with at least 200 cells counted from each slide.

BAL and plasma biochemistry. All biochemical assays were modified to be assessed on a Konelab 30 clinical chemistry analyzer from

Thermo Clinical Labsystems. Activity for lactate dehydrogenase (LDH) and N-Acetyl-β-D-glucosaminase (NAG) were determined using commercially available kits from Sigma, (MO). Total protein concentrations were determined with the Coomassie plus protein assay (Pierce Chemical, IL). Pro-inflammatory cytokines macrophage inflammatory protein 2 (MIP-2), tumor necrosis factor alpha (TNF-α) and interleukin-6 (IL-6) concentrations in BAL were measured by ELISA using mouse Quantikine kits purchased form Biosource (Camarillo, CA). For the plasma analyses, kits for creatine kinase (CK) and amino-S-transferase (AST) were obtained from Thermo Electron, Melbourne, Australia. Kits and standards for C-reactive protein (CRP) and fibrinogen (FIB) were obtained from DiaSorin Inc., Stillwater, MN, except the standard for the CRP was a mouse reference serum standard with a known concentration (Kamiya Biomedical Company, Seattle, WA).

Cardiac perfusion. A separate group of mice was used for cardiac perfusion as described previously (Tong et al., 2005). 24 hours after instillation, mice were anesthetized with 0.1 ml of a 10:1 pentobarbital solution and weighed. Heparin (100 U) was injected intravenously before removal of the heart. The hearts were rapidly excised and placed in ice-cold Krebs–Henseleit buffer, and the aortas were cannulated. Retrograde perfusion was under constant perfusion pressure of 100 cm above the heart. The non-recirculating perfusate

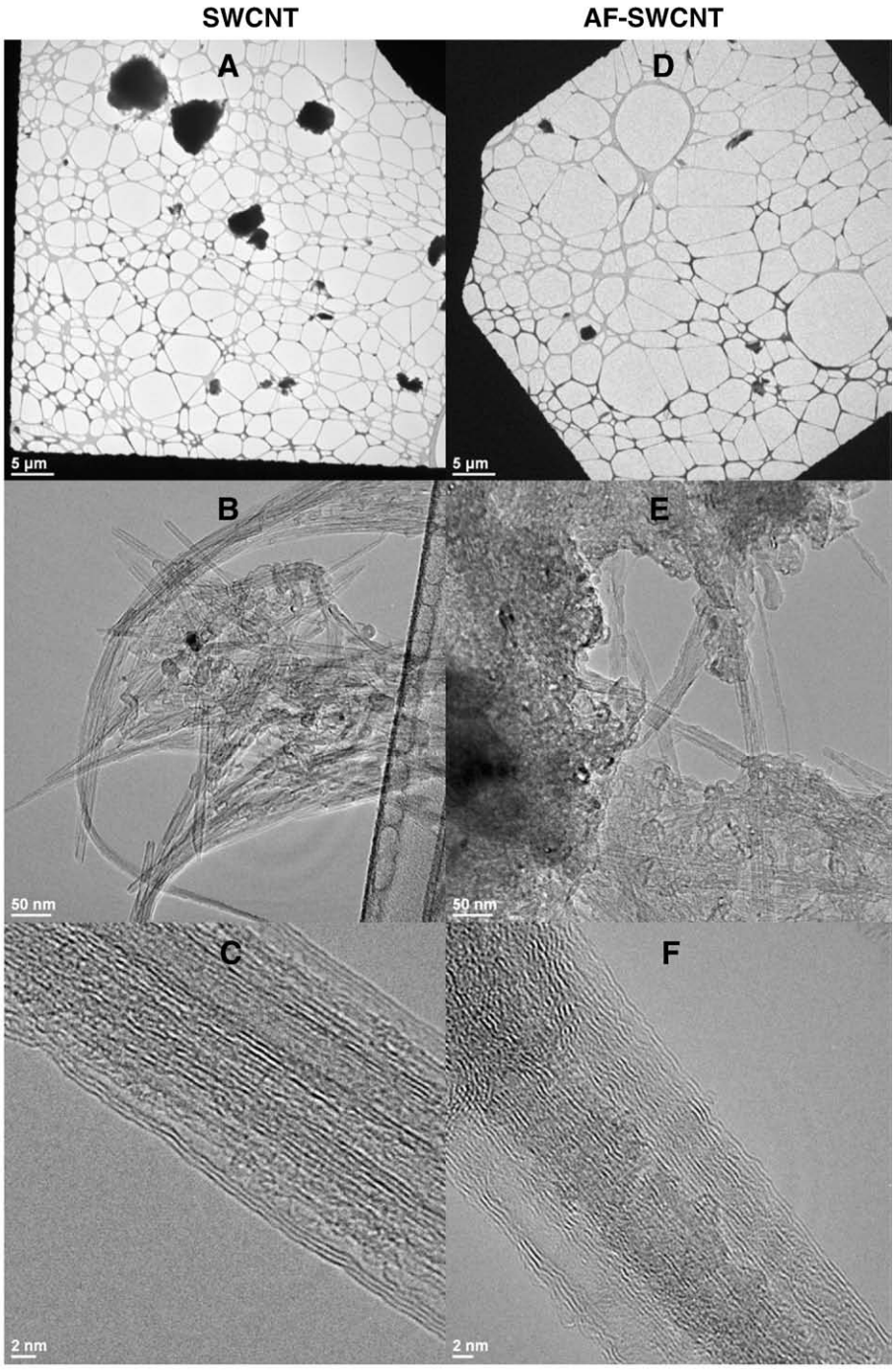

Fig. 1. TEM images of SWCNT and AF-SWCNT. Panels A and D show bulk solids as agglomerates, note size reduced to <5 μm for AF-SWCNT. Panels B and E show high-resolution details of individual nanotubes in the agglomerates and Panels C and F depict individual nanotubes, note roughened edges of AF-SWCNT sidewalls.

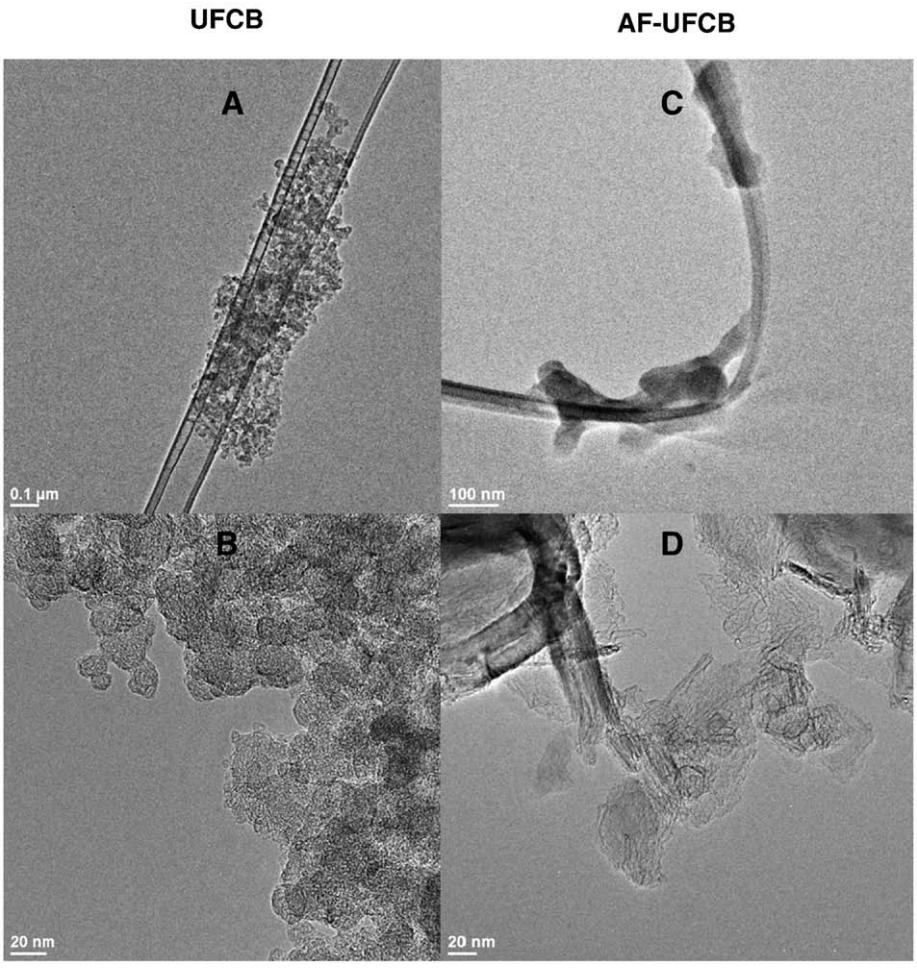

Fig. 2. TEM images of UFCB and AF-UFCB. Panels A and C show the typical agglomerate structure of the parent material, as well as greatly modified surface of AF-UFCB. Panels B and D show high-resolution details of individual particles; note that AF-UFCB is now merged into larger forms with greatly reduced surface area.

was a Krebs–Henseleit buffer containing 120 NaCl, 5.9 KCl, 1.2 $MgSO_4$, 1.75 $CaCl_2$, 25 $NaHCO_3$, and 11 mmol/l glucose. The buffer was aerated with 95% O_2–5% CO_2 and maintained at pH 7.4 and a temperature of 37 °C.

For assessment of contractile function, a latex balloon on the tip of a polyethylene catheter was inserted through the left atrium into the left ventricle. The catheter was connected to a pressure transducer (Argon; Athens, TX) at the same height as the heart. A PowerLab system was used to collect and process the left ventricular pressure data (AD Instruments; Milford, MA). Hearts that did not achieve a developed pressure of at least 90 cmH_2O were excluded. All hearts were perfused for 25 min prior to the start of a 20 min-no-flow ischemia followed by 2 h of reperfusion. Coronary flow rate was measured before and after ischemia by collecting the effluent from the heart. Recovery of post-ischemic left ventricular developed pressure (LVDP), expressed as a percentage of the initial preischemic LVDP was measured at 1 h of reperfusion after 20-min of ischemia.

Cardiac necrosis evaluation. At the end of 2 h of reperfusion, hearts were perfused with 15 ml of 1% solution of 2,3,5-triphenyltetrazolium chloride (TTC) dissolved in Krebs–Henseleit buffer, then incubated in 1% TTC at 37 °C for 10 min, and then fixed in formalin. The area of necrosis was measured by taking cross-sectional slices through the ventricles, which were then photographed using a digital camera mounted on a stereo-microscope. The resulting images were quantified by measuring the areas of stained versus unstained tissue with the use of Adobe Photoshop. Infarct size was expressed as a percentage of the whole heart.

Histology. To further characterize injury and inflammation in hearts and lungs, and to monitor for the presence of particles in each tissue, additional groups of animals were necropsied at 24 h. The trachea was cannulated, the lungs removed and inflated in 10% formalin at 20 cm of H_2O pressure. Following embedding and processing, all lung lobes were sectioned along a mid-saggital plane into 4–6 μm sections, and

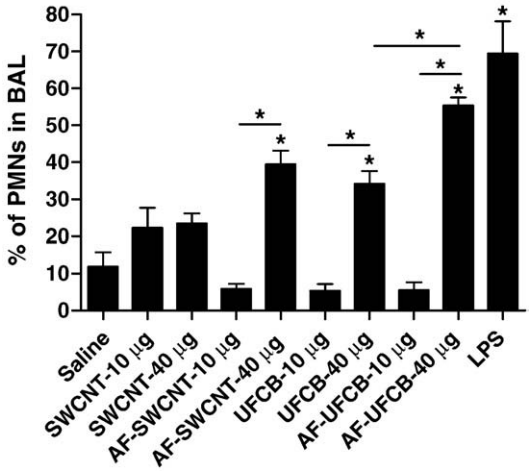

Fig. 3. Percent of neutrophils in BAL fluid of mice 24 h after particle instillation. Values are means ± SE ($n = 13$ in saline group, $n = 8$ in 40 μg of AF-SWCNT group, $n = 9$ in LPS group, $n = 10$ in other 40 μg groups, and $n = 5$ in all 10 μg groups). *$p < 0.05$ compared with saline group or between two groups.

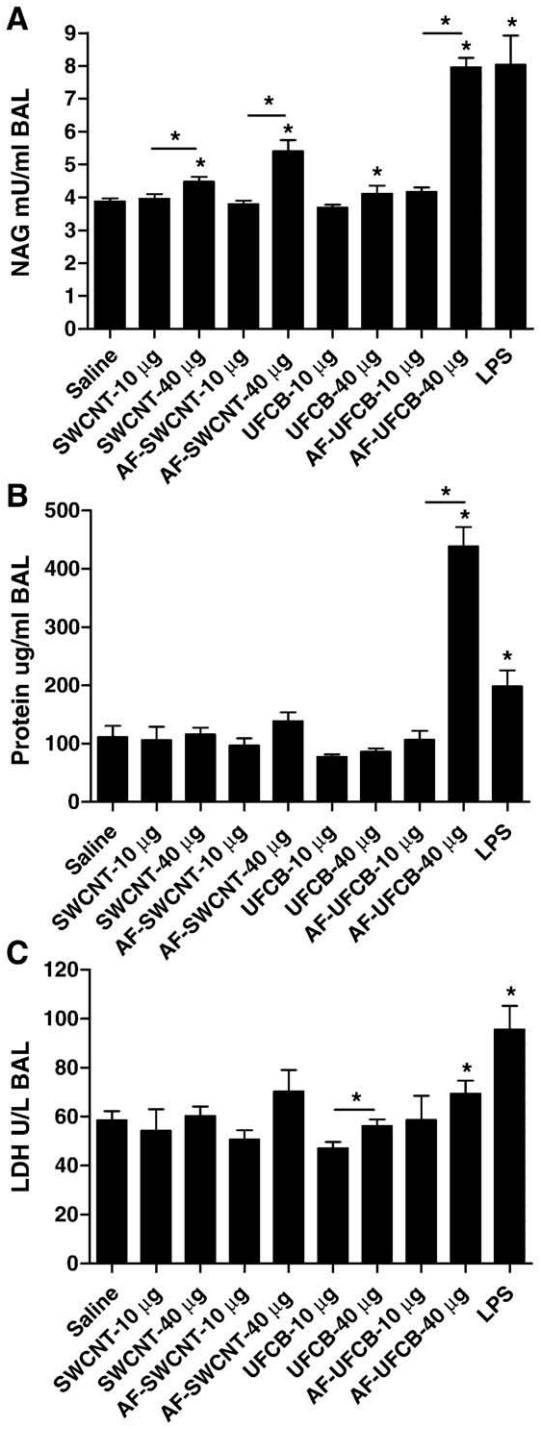

Fig. 4. Concentration of NAG, protein and LDH in BAL fluid of mice 24 h after particle instillation. Values are means ± SE ($n = 13$ in saline group, $n = 8$ in 40 μg of AF-SWCNT group, $n = 9$ in LPS group, and $n = 10$ in other 40 μg groups, and $n = 5$ in all 10 μg groups). *$p < 0.05$ compared with saline group or between two groups.

stained with hematoxylin and eosin. Lung sections were assessed at 200× for signs of inflammation, injury and presence of particles. Likewise hearts were fixed in 10% formalin, cut longitudinally to obtain representative sections of left and right ventricles, embedded in paraffin blocks, sectioned into 4–6 μm sections, and stained with hematoxylin and eosin or trichrome. Functional studies demonstrated that only the 40 μg of AF-SWCNT exposure enhanced cardiac ischemia/reperfusion injury, therefore the cardiac histological study was performed between this and the saline group. Sections were viewed under light microscopy (1000×) and cardiac lesions were scored in a blinded fashion by a Board Certified Veterinary Pathologist (Experimental Pathology Laboratories, RTP, NC) using grades 1 (minimal) to 5 (severe) based on the number of affected cells and size of cell clusters.

Statistical analysis. Data are expressed as means ± SE. One-way ANOVA was used to compare the differences, followed by Tukey's post hoc test for multiple comparisons. The statistical significance level was set at $p < 0.05$.

Results

Effect of acid functionalization on the physico-chemical properties of SWCNT and UFCB

Elemental analysis in Table 1 showed that acid functionalization of SWCNT lowered carbon content by 20% and the transition metals Co, Cr, Fe, Mn, and Ni contents to a similar extent (24–33%). This is consistent with mild sulfonation/carboxylation addition to the nanotube sidewalls while leaving the basic nanotube structure unchanged (Wang et al., 2006). Mo content of AF-SWCNT was substantially decreased indicating either greater solubility of this element or improved accessibility to acids during functionalization. Al, Ca, SiO_2, and Zn content increased slightly in AF-SWCNT, as artifacts from neutralization and dialysis steps during preparation. Particle size distributions of AF-SWCNT aqueous suspensions obtained from the zetasizer instrument showed that >95% were in the range between 22 and 138 nm. Fig. 1 shows TEM images of both SWCNT and AF-SWCNT. Panels A and D show both bulk solids as agglomerates, with the size reduced to <5 μm for AF-SWCNT. Panels B and E show high-resolution details of individual nanotubes in the agglomerates, and panels C and F depict individual nanotubes. As described previously (Wang et al., 2006), acid functionalization effects were noticeable by the roughened sidewalls of AF-SWCNT. BET surface area of AF-SWCNT was one-third that of SWCNT (Table 1). Reduction of surface area of functionalized SWCNT bulk solids is common and believed to result from nanotube rebundling (Chakraborty et al., 2006) during preparation, most likely in the drying step.

UFCB was mostly elemental carbon with little inorganic content, as confirmed by elemental analysis. Acid functionalization reduced UFCB carbon content by approximately 50%, while the inorganic content was moderately increased. TEM pictures in panels A and C of Fig. 2 show the typical agglomerate structure of the parent material, as well as the greatly modified surface of the AF-UFCB. Panels B and D and the BET values (Table 1) of UFCB and AF-UFCB confirmed that the acid functionalization resulted in significant agglomeration of the UFCB with an accompanying greatly reduced surface area. Aqueous resuspension of AF-UFCB however resulted in >95% between 71 and 96 nm as recorded by the zetasizer, indicating that the acid functionalization did not affect the size of the parent material.

Table 2
Total white blood cells, red blood cells, lymphocytes, and platelets count 24 h after particles exposure.

	n	WBC ($\times 10^3/\mu l$)	Platelets ($\times 10^3/\mu l$)	RBC ($\times 10^6/\mu l$)	Lymphocytes ($\times 10^3/\mu l$)
Saline	6	3.32 ± 0.33	1007 ± 167	7.32 ± 0.22	2.82 ± 0.37
40 μg SWNT	6	2.58 ± 0.23	1186 ± 117	6.87 ± 0.18	2.03 ± 0.20
40 μg AF-SWNT	6	2.53 ± 0.40	1212 ± 65	6.73 ± 0.17*	2.10 ± 0.35
40 μg UFCB	6	2.98 ± 0.53	1172 ± 98	6.58 ± 0.11*	2.85 ± 0.53
40 μg AF-UFCB	6	2.72 ± 0.25	1277 ± 92	6.76±0.21	2.11 ± 0.18
LPS	6	2.97 ± 0.32	1180 ± 99	6.98 ± 0.18	2.00 ± 0.24

Values are mean ± SE.
* $p < 0.05$ compared to saline group.

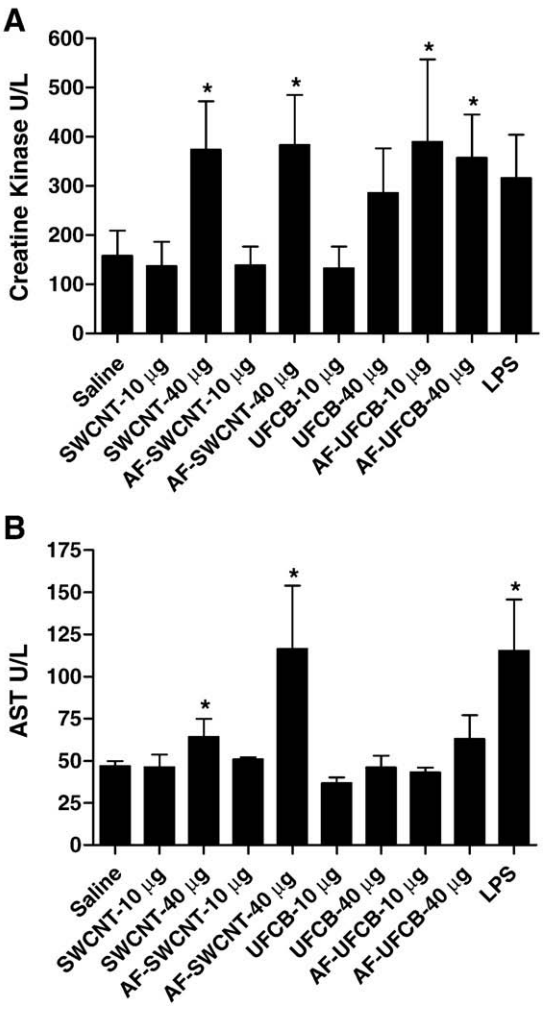

Fig. 5. Plasma creatine kinase and AST levels in mice 24 h after particle instillation. Values are means ± SE ($n = 13$ in saline group, $n = 8$ in 40 μg of AF-SWCNT group, $n = 9$ in LPS group, $n = 10$ in other 40 μg groups, and $n = 5$ in all 10 μg groups). *$p < 0.05$ compared with saline group.

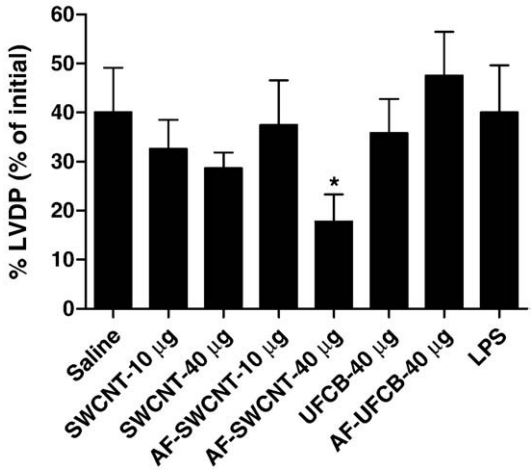

Fig. 6. Recovery of LVDP measured at 1 h of reflow after 20 min of ischemia. Values are means ± SE ($n = 7$ in saline group, $n = 5$ in LPS and 10 μg or 40 μg of SWCNT and AF-SWCNT groups, and $n = 4$ in 40 μg of UFCB and AF-UFCB groups). *$p < 0.05$ compared with saline hearts.

Pulmonary toxicity

To determine whether the particles affected pulmonary inflammatory responses, mice were exposed to each of the different particle types, and saline and LPS as negative and positive controls respectively. As expected, LPS caused the greatest increase in percent of PMNs which was significantly higher than all particle-exposed groups. There were significant increases in the percentage of BAL neutrophils from mice exposed to 40 μg of AF-SWCNT or the UFCB and the AF-UFCB compared to saline group (Fig. 3). Neutrophils were also significantly greater in mice exposed to 40 μg of AF-UFCB compared to the non-functionalized particles. No significant changes were seen with the lower concentration of particles. Assessment of lung histology samples in the 40 μg exposure groups revealed sporadic clumps of free black particulate in some of the small airways with less material noted in the acid-functionalized preparations. Black particulate matter was also evident in focal areas of the interstitium and appeared to be intracellular. Again, less material was detected with the AF treatment, although in all groups the particulate was infrequently seen under several fields at 200×. In agreement with the inflammation data, the high dose particle exposures resulted in cellular infiltration which was apparent in the alveolar spaces and around the small airways. The lung interstitium was slightly edematous in areas where cellular accumulation was evident.

In addition to neutrophils, LPS significantly increased LDH, protein, and NAG (as markers of injury, edema, and cellular activation respectively) in BAL fluid compared to the saline group (Fig. 4). Mice exposed to 40 μg of SWCNT, AF-SWCNT, UFCB, and AF-UFCB had significantly increased levels of NAG in BAL fluid and this was higher in the AF-UFCB compared to the UFCB. Mice exposed to AF-UFCB also had the highest levels of BAL protein, while mice exposed to 40 μg of AF-UFCB had more LDH release than the saline controls and the other UFCB groups. Cytokine levels in all BAL samples were outside the detection limits of the assay and could not be repeated because of lack of additional sample (data not shown).

Systemic effects

Examination of systemic inflammatory and coagulation effects revealed slight decreases in red blood cells which were significant

Table 3
Pre-ischemic hemodynamic properties and the onset time to ischemic contracture.

	n	LVDP (mm Hg)	HR (bpm)	Flow rate (ml/min)	dP/dT-max	dP/dT-min	Time to contracture (min)
Saline	7	130 ± 12	401 ± 21	3.0 ± 0.2	3934 ± 342	−3612 ± 314	9.3 ± 0.9
10 μg SWCNT	5	109 ± 8	380 ± 21	2.6 ± 0.4	4007 ± 274	−2898 ± 411	12.2 ± 2.0
40 μg SWCNT	5	122 ± 12	408 ± 42	3.4 ± 0.4	3103 ± 230	−3137 ± 453	8.0 ± 1.1
10 μg AF-SWCNT	5	116 ± 9	395 ± 9	2.8 ± 0.7	4391 ± 370	−2958 ± 511	10.8 ± 1.1
40 μg AF-SWCNT	5	152 ± 17	424 ± 28	6.2 ± 0.4*	3780 ± 416	−3779 ± 593	5.2 ± 0.6*
40 μg UFCB	4	169 ± 30	409 ± 8	3.2 ± 0.4	5224 ± 988	−4224 ± 555	8.0 ± 1.2
40 μg AF-UFCB	4	148 ± 16	424 ± 12	3.3 ± 0.6	4932 ± 730	−3536 ± 278	8.5 ± 1.3
LPS	5	129 ± 15	395 ± 41	3.0 ± 0.4	4372 ± 411	−3329 ± 639	11.2 ± 1.9

Values are means ± SE. LVDP = left ventricular developed pressure; HR = heart rate; flow rate = coronary flow rate; dP/dT-max = maximum 1st derivative of the change in left ventricular pressure/time; dP/dT-min = minimum 1st derivative of the change in left ventricular pressure/time; time to contracture = onset time to ischemic contracture.
* $p < 0.01$ compared to saline group.

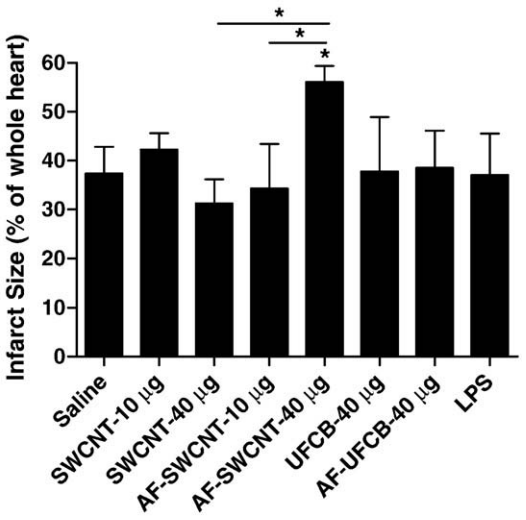

Fig. 7. Infarct size measured using TTC staining at 2 h of reflow after 20 min of ischemia. Values are means ± SE ($n = 7$ in saline group, $n = 5$ in LPS and 10 μg and 40 μg of SWCNT and AF-SWCNT groups, and $n = 4$ in 40 μg of UFCB and AF-UFCB groups). *$p<0.05$ compared with saline group or between two groups.

in the mice exposed to 40 μg of AF-SWCNT and UFCB (Table 2). There was a significant increase in plasma creatine kinase in mice exposed to 40 μg of SWCNT and AF-SWCNT, and mice exposed to both 10 μg and 40 μg of AF-UFCB (Fig. 5A). Aspartate aminotransferase (AST) was also increased in mice exposed to 40 μg of SWCNT and AF-SWCNT (Fig. 5B). There was no significant difference between acid-functionalized and non-functionalized groups in creatine kinase and AST levels. There were no differences in plasma C-reactive protein (CRP) and fibrinogen levels between any of the exposures (data not shown).

Cardiac ischemic/reperfusion injury

There were no significant changes in baseline LVDP, heart rate, $+dP/dt_{max}$, and $-dP/dt_{min}$ after the 24 h particle exposure (Table 3). The coronary flow rate in mice exposed to 40 μg of AF-SWCNT group was significantly higher than that of the other groups (Table 3). This exposure also resulted in earlier ischemic contracture (5 ± 1 min for 40 μg of AF-SWCNT versus 9 ± 1 min for saline control; $p<0.01$) (Table 3).

Hearts from the 40 μg of AF-SWCNT-exposed mice showed significantly lower recovery of post-ischemic LVDP compared to hearts from saline, 10 μg of AF-SWCNT, LPS, and acid-functionalized and non-functionalized UFCB-exposed mice (Fig. 6). Neither UFCB nor AF-UFCB diminished recovery of post-ischemic LVDP. Mice exposed to 40 μg of AF-SWCNT demonstrated a significantly increased infarct size compared to saline. This effect was also significantly greater than the 10 μg of AF-SWCNT and 40 μg of SWCNT groups (Fig. 7). Animals given LPS did not show any significant changes, suggesting that the increased myocardial ischemic injury by 40 μg of AF-SWCNT was not caused by pulmonary inflammation since this was even higher in the LPS and 40 μg dose of AF-UFCB groups.

Myocardial degeneration

Cardiac histology showed that myofiber degeneration was more commonly observed in hearts from mice exposed to 40 μg of the AF-SWCNT group than the saline group. Hematoxylin and eosin staining (Fig. 8C) revealed small clusters of myocytes that were shrunken, rounded, hypereosinophilic, and contained pyknotic nuclei in the papillary muscle and interventricular septum in the AF-SWCNT exposed hearts. In contrast, the myocytes were longitudinally striated in the saline hearts (Fig. 8A). Trichrome staining (Fig. 8D) showed that the affected myocytes stained prominently red with variable streaks of blue stain within degenerative foci in the AF-SWCNT hearts. In a few

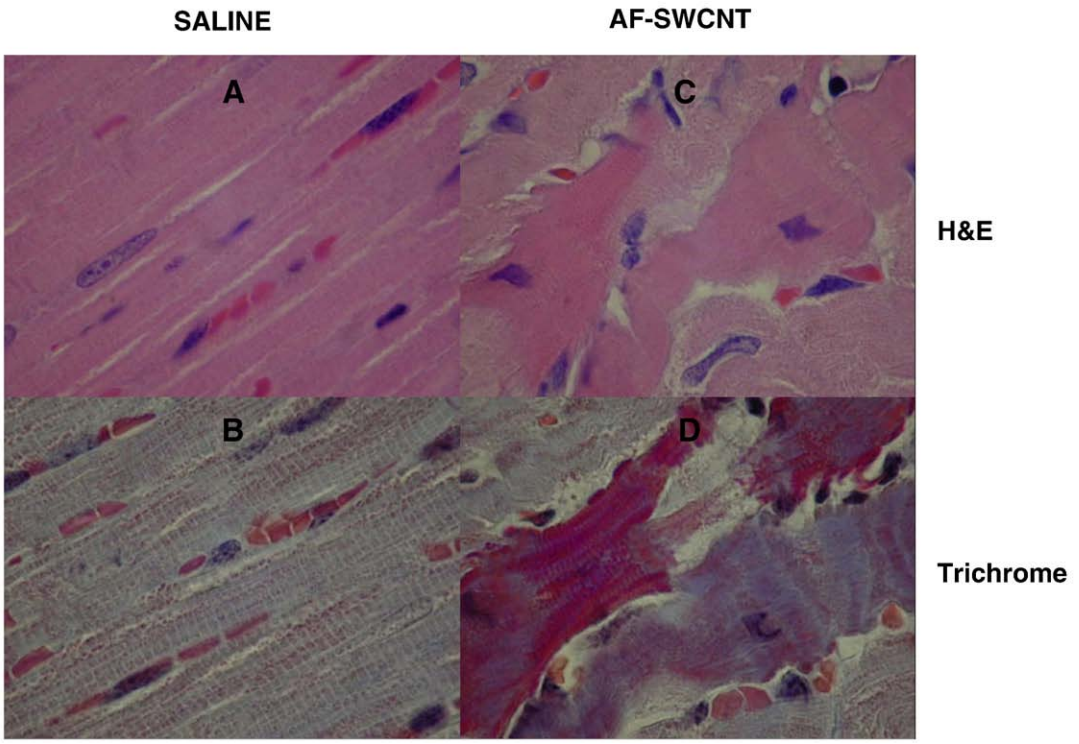

Fig. 8. Cardiac myofiber degeneration in mouse hearts 24 h after 40 μg of AF-SWCNTs exposure with hematoxylin and eosin (C) and trichrome staining (D). Focal degenerating myocytes are round and shrunken (C and D) compared to the normal myocytes that are longitudinally striated (A and B). Representative sections of the myocardium from saline (A and B) and AF-SWCNTs (C and D) exposed mice are shown (1000×). Each photomicrograph represents a section from an individual heart.

myocytes, the blue stain coalesced and resembled contraction bands. The lesions were scored using grades 1 (minimal) to 5 (severe) based on the number of affected cells and size of cell clusters. An average severity score of 1 was recorded in the 40 μg of the AF-SWCNT group compared to 0 for the saline group (4 hearts per treatment).

Discussion

Acid functionalization has been proposed as a useful technique to improve the solubility and dispersion of highly aggregated materials such as carbon nanotubes (Wang et al., 2006). We have previously demonstrated that this process increases the *in vitro* and *in vivo* toxicity of carbon nanotubes (on a mass basis), and that this effect can be reversed by neutralizing the surface charge, which in turn reduces dispersion (Saxena et al., 2007). In this study we investigated whether SWCNT could cause cardiac toxicity following acute pulmonary exposure in animals, and if chemically modifying these particles would affect the outcome. The results showed that the acid-functionalized carbon nanotubes (AF)-SWCNTs increased cardiac ischemia/reperfusion injury as evidenced by the decreased recovery of cardiac function, increased infarct size and mild cardiac myofiber degeneration. To confirm whether the addition of functional groups was responsible for this effect, other groups of animals were exposed to carbon black with and without this treatment. Although the AF-UFCB particles produced even higher pulmonary inflammatory responses, they did not affect ischemia/reperfusion injury in the hearts compared to the UFCB or saline controls. This would suggest that functionalization alone was not sufficient to cause cardiac injury, and that both the nanotubular structure and reactive surface appeared to be required.

Acid functionalization greatly reduced the surface area of both the carbon black particles and carbon nanotubes, while causing stronger pulmonary inflammatory effects as noted in our earlier report (Saxena et al., 2007). Although the toxicity of particles generally increases with surface area (Oberdorster et al., 2005; Stoeger et al., 2006), the addition of functional reactive groups could also increase the inflammatory potential while effectively decreasing surface area through alterations in physical chemistry. The decreased surface area following the functionalization process confirms previous reports which suggested that this occurred, either through rebundling of the nanotubes (Chakraborty et al., 2006), or in the case of carbon black, by oxygenated groups blocking the micropores on particles (Carmo et al., 2009).

The increased cardiac toxicity due to functionalization process was likely caused either by improved translocation of particles to the circulation, or by the release of endogenous mediators that subsequently affected cardiovascular functions. It has been reported that ultrafine particles can translocate from the lung to the systemic circulation by crossing the alveolar–capillary barrier (Nemmar et al., 2001; Oberdorster et al., 2002). This could cause direct cardiovascular effects including systemic inflammation, endothelial injury, and activation of coagulation pathways and thrombus development (Radomski et al., 2005). It has been reported that carbon nanotubes damaged the endothelial cells with a resultant increase in permeability *in vitro* (Walker et al., 2009).

Although translocation of particles was not demonstrated here, the increased solubility and dispersion of AF-SWCNT could have enhanced potential for this to occur. In addition, the increased coronary flow rate in the AF-SWCNT-exposed mice could have contributed to greater particle movement through the vasculature and may in fact have been a result of increased permeability. Furthermore, the early onset of ischemic contracture in the AF-SWCNT-exposed hearts suggested that the myocardium was predisposed to the ischemic insult possibly through depletion of cellular ATP as previously described (Steenbergen et al., 1990).

Enhanced cardiac ischemia/reperfusion injury was not found in mice exposed to AF-UFCB, suggesting that the surface chemistry was important for the cardiac toxicity of AF-SWCNT. It is possible that carbon black was either cleared from the lung through mucociliary clearance or did not enter the interstitial space as readily as the SWCNT particles. Radiotracer imaging techniques have reported that 75% of ultrafine carbon particles are retained in human airways without substantial systemic translocation and clearance (Moller et al., 2008), or accumulation in the liver and spleen (Mills et al., 2006). Comparison of the pulmonary toxicity between SWCNTs and UFCB however, found the fate of particles and reaction with lung tissues to be very different (Lam et al., 2004). The lungs appeared to be normal histologically in mice exposed to UFCB except for the presence of particle-laden macrophages (Lam et al., 2004). In contrast, epithelioid granulomas developed in the lungs 7 days after treated with SWCNTs, indicating that the particles entered the interstitial space and were not cleared (Lam et al., 2004). This would suggest that nanotubes (but not ultrafine carbon black particles) have the ability to penetrate or to be taken up in tissue and that acid functionalization could accelerate this process thus enhancing the potential for cardiac toxicity.

Indirect processes may also be responsible for the cardiac effects induced by AF-SWCNT exposure. Although the AF-SWCNT-induced cardiac effects could have resulted from particle-initiated pulmonary and systemic inflammation, the higher responses observed with LPS and AF-UFCB treated mice in the absence of significant cardiac effects would argue against this mechanism. It is however still possible that the unique nature of the AF-SWCNTs caused the release of specific vasoactive mediators which were responsible for later cardiovascular dysfunction. The increased coronary flow rate could also have resulted from AF-SWCNT-induced vasodilatation of the coronary vasculature. Finally, although it was not tested in the present study, the cardiac effects of AF-SWCNTs could have been mediated through nanotube-induced oxidative stress. It has been demonstrated that nanoparticles preferentially mobilize to mitochondria (Savic et al., 2003). In addition, pulmonary exposure to SWCNTs has been associated with oxidative vascular damage in wild type mice, as well as accelerated atherosclerosis in ApoE$^{-/-}$ transgenic mice in the absence of systemic inflammation (Li et al., 2007). Further studies to examine the cardiac effects from oxidative stress in AF-SWCNT-exposed animals are warranted.

Conclusions

Intrapulmonary instillation of acid-functionalized SWCNTs enhanced cardiac ischemia/reperfusion injury and caused myocardial degeneration in mice. There was no significant ischemia/reperfusion injury in mice exposed to non-functionalized SWCNTs or ultrafine carbon particles, despite significant pulmonary inflammation, suggesting that the combination of acid functionalization and SWCNTs was required to mediate extra-pulmonary toxicity. Further studies are required to determine whether this effect was due to enhanced translocation, or via systemic vascular response generated in association with the AF-SWCNT-mediated pulmonary injury.

Funding

The research described was supported by the US EPA Intramural Federal Research.

Acknowledgments

We thank Mary Daniels, Elizabeth Boykin, Judy Richards and Richard Jaskot, Laura Degn, Mike McClure for excellent technical assistance, and Drs. Mary Jane Selgrade, Linda Birnbaum and Aimen Farraj for their review of this manuscript. We also thank Naresh Shah for supplying TEM images and Stephen Rankin for BET surface area determinations, both from the University of Kentucky. This paper has

been reviewed by the National Health and Environmental Effects Research Laboratory, US Environmental Protection Agency, and approved for publication. The contents of this article should not be construed to represent Agency policy nor does mention of trade names or commercial products constitute endorsement or recommendation for use.

References

Aitken, R.J., Chaudhry, M.Q., Boxall, A.B., Hull, M., 2006. Manufacture and use of nanomaterials: current status in the UK and global trends. Occup. Med. (Lond) 56, 300–306.

Ajima, K., Yudasaka, M., Murakami, T., Maigne, A., Shiba, K., Iijima, S., 2005. Carbon nanohorns as anticancer drug carriers. Mol. Pharm. 2, 475–480.

Bianco, A., Hoebeke, J., Kostarelos, K., Prato, M., Partidos, C.D., 2005. Carbon nanotubes: on the road to deliver. Curr. Drug Deliv. 2, 253–259.

Carmo, M., Linardi, M., Rocha poco, J., 2009. Characterization of nitric acid functionalized carbon black and its evaluation as electrocatalyst support for direct methanol fuel cell applications. Applied Catalysis A: General 355, 132–138.

Chakraborty, S., Chattopadhyay, J., Peng, H., Chen, Z., Mukherjee, A., Arvidson, R.S., Hauge, R.H., Billups, W.E., 2006. Surface area measurement of functionalized single-walled carbon nanotubes. J. Phys. Chem. B. 110, 24812–24815.

Cozzi, E., Hazarika, S., Stallings 3rd, H.W., Cascio, W.E., Devlin, R.B., Lust, R.M., Wingard, C.J., Van Scott, M.R., 2006. Ultrafine particulate matter exposure augments ischemia-reperfusion injury in mice. Am. J. Physiol. Heart Circ. Physiol. 291, H894–903.

Gilmour, M.I., O Connor, S., Dick, C.A., Miller, C.A., Linak, W.P., 2004. Differential pulmonary inflammation and in vitro cytotoxicity of size-fractionated fly ash particles from pulverized coal combustion. J. Air. Waste Manag. Assoc. 54, 286–295.

Helland, A., Wick, P., Koehler, A., Schmid, K., Som, C., 2007. Reviewing the environmental and human health knowledge base of carbon nanotubes. Environ. Health Perspect. 115, 1125–1131.

Lam, C.W., James, J.T., McCluskey, R., Hunter, R.L., 2004. Pulmonary toxicity of single-wall carbon nanotubes in mice 7 and 90 days after intratracheal instillation. Toxicol. Sci. 77, 126–134.

Lam, C.W., James, J.T., McCluskey, R., Arepalli, S., Hunter, R.L., 2006. A review of carbon nanotube toxicity and assessment of potential occupational and environmental health risks. Crit. Rev. Toxicol. 36, 189–217.

Li, Y.H., Di, Z., Ding, J., Wu, D., Luan, Z., Zhu, Y., 2005. Adsorption thermodynamic, kinetic and desorption studies of Pb2+ on carbon nanotubes. Water Res. 39, 605–609.

Li, Z., Hulderman, T., Salmen, R., Chapman, R., Leonard, S.S., Young, S.H., Shvedova, A., Luster, M.I., Simeonova, P.P., 2007. Cardiovascular effects of pulmonary exposure to single-wall carbon nanotubes. Environ. Health Perspect. 115, 377–382.

Mills, N.L., Amin, N., Robinson, S.D., Anand, A., Davies, J., Patel, D., de la Fuente, J.M., Cassee, F. R., Boon, N.A., Macnee, W., Millar, A.M., Donaldson, K., Newby, D.E., 2006. Do inhaled carbon nanoparticles translocate directly into the circulation in humans? Am. J. Respir. Crit. Care Med. 173, 426–431.

Moller, W., Felten, K., Sommerer, K., Scheuch, G., Meyer, G., Meyer, P., Haussinger, K., Kreyling, W.G., 2008. Deposition, retention, and translocation of ultrafine particles from the central airways and lung periphery. Am. J. Respir. Crit. Care Med. 177, 426–432.

Nemmar, A., Vanbilloen, H., Hoylaerts, M.F., Hoet, P.H., Verbruggen, A., Nemery, B., 2001. Passage of intratracheally instilled ultrafine particles from the lung into the systemic circulation in hamster. Am. J. Respir. Crit. Care Med. 164, 1665–1668.

Oberdorster, G., Sharp, Z., Atudorei, V., Elder, A., Gelein, R., Lunts, A., Kreyling, W., Cox, C., 2002. Extrapulmonary translocation of ultrafine carbon particles following whole-body inhalation exposure of rats. J. Toxicol. Environ. Health A. 65, 1531–1543.

Oberdorster, G., Oberdorster, E., Oberdorster, J., 2005. Nanotoxicology: an emerging discipline evolving from studies of ultrafine particles. Environ. Health Perspect. 113, 823–839.

Radomski, A., Jurasz, P., Alonso-Escolano, D., Drews, M., Morandi, M., Malinski, T., Radomski, M.W., 2005. Nanoparticle-induced platelet aggregation and vascular thrombosis. Br. J. Pharmacol. 146, 882–893.

Savic, R., Luo, L., Eisenberg, A., Maysinger, D., 2003. Micellar nanocontainers distribute to defined cytoplasmic organelles. Science 300, 615–618.

Saxena, R.K., Williams, W., McGee, J.K., Daniels, M.J., Boykin, E., Gilmour, M.I., 2007. Enhanced in vitro and in vivo toxicity of poly-dispersed acid-functionalized single-wall carbon nanotubes. Nanotoxicology 1 (4), 291–300.

Schulz, H., Harder, V., Ibald-Mulli, A., Khandoga, A., Koenig, W., Krombach, F., Radykewicz, R., Stampfl, A., Thorand, B., Peters, A., 2005. Cardiovascular effects of fine and ultrafine particles. J. Aerosol. Med. 18, 1–22.

Shvedova, A.A., Kisin, E., Murray, A.R., Johnson, V.J., Gorelik, O., Arepalli, S., Hubbs, A.F., Mercer, R.R., Keohavong, P., Sussman, N., Jin, J., Yin, J., Stone, S., Chen, B.T., Deye, G., Maynard, A., Castranova, V., Baron, P.A., Kagan, V.E., 2008. Inhalation vs. aspiration of single-walled carbon nanotubes in C57BL/6 mice: inflammation, fibrosis, oxidative stress, and mutagenesis. Am. J. Physiol. Lung Cell. Mol. Physiol. 295, L552–565.

Singh, R., Pantarotto, D., Lacerda, L., Pastorin, G., Klumpp, C., Prato, M., Bianco, A., Kostarelos, K., 2006. Tissue biodistribution and blood clearance rates of intravenously administered carbon nanotube radiotracers. Proc. Natl. Acad. Sci. U. S. A. 103, 3357–3362.

Steenbergen, C., Murphy, E., Watts, J.A., London, R.E., 1990. Correlation between cytosolic free calcium, contracture, ATP, and irreversible ischemic injury in perfused rat heart. Circ. Res. 66, 135–146.

Stern, S.T., McNeil, S.E., 2008. Nanotechnology safety concerns revisited. Toxicol. Sci. 101, 4–21.

Stoeger, T., Reinhard, C., Takenaka, S., Schroeppel, A., Karg, E., Ritter, B., Heyder, J., Schulz, H., 2006. Instillation of six different ultrafine carbon particles indicates a surface area threshold dose for acute lung inflammation in mice. Environ. Health Perspect. 114, 328–333.

Tong, H., Bernstein, D., Murphy, E., Steenbergen, C., 2005. The role of beta-adrenergic receptor signaling in cardioprotection. FASEB J. 19, 983–985.

Walker, V.G., Li, Z., Hulderman, T., Schwegler-Berry, D., Kashon, M.L., Simeonova, P.P., 2009. Potential in vitro effects of carbon nanotubes on human aortic endothelial cells. Toxicol. Appl. Pharmacol. 236, 319–328.

Wang, Y., Iqbal, Z., Mitra, S., 2006. Rapidly functionalized, water-dispersed carbon nanotubes at high concentration. J. Am. Chem. Soc. 128, 95–99.

Wick, P., Manser, P., Limbach, L.K., Dettlaff-Weglikowska, U., Krumeich, F., Roth, S., Stark, W.J., Bruinink, A., 2007. The degree and kind of agglomeration affect carbon nanotube cytotoxicity. Toxicol. Lett. 168, 121–131.